Sputtered W–N diffusion barriers*

H. P. Kattelus,[a] E. Kolawa, K. Affolter, and M-A. Nicolet
California Institute of Technology, Pasadena, California 91125

(Received 30 April 1985; accepted 3 June 1985)

The thermal stability of reactively sputtered tungsten–nitrogen alloy thin films is investigated for the application as diffusion barriers in silicon contact metallizations. The composition of W–N barriers is varied over a wide range including pure W. Aluminum, gold, and silver are used as low resistivity overlayers. Metallurgical interactions at temperatures ranging from 500 to 900 °C are studied. Incorporating nitrogen into tungsten advantageously stabilizes all three systems. The overall failure takes place rapidly above critical temperatures that depend on both the metal overlayer and the microstructure of the barrier. In some cases, W–N alloys can effectively prevent interdiffusion at temperatures as high as 800 °C for 30 min.

I. INTRODUCTION

Tungsten is a widely used element in semiconductor contacting technology. First, tungsten serves as a single layer metallization replacing the conventional aluminum metallization on silicon. The breakthrough of tungsten in this application is largely due to the advantages of chemical vapor deposition that is now routinely used to grow tungsten layers.[1] Second, the disilicide of tungsten forms a reliable electrical contact to silicon, and it decreases the sheet resistance of polycrystalline silicon in "polycide" structures.[2] Third, tungsten is a constituent element in various diffusion barriers that are used to retard the interactions of silicon or its contacting silicide with a metal overlayer.[3] It is this diffusion barrier aspect that is considered here.

An ideal diffusion barrier for a contact metallization is a chemically and mechanically stable and electrically conductive layer that inhibits interdiffusion between its bordering media.[4] Most of the metallic elements have proved to be unsatisfactory for high temperature diffusion barrier applications because of intermetallic compound formation, of finite solubility between the neighboring materials, or of rapid grain boundary motion of atoms through the barrier. Tungsten, when applied as an elemental barrier layer, shows strongly varying properties from one study to another.[5–8] The differences may well be related to the impurity content of the layers, because it has been shown that properties of polycrystalline barriers can be changed much by "stuffing" the grain boundaries with elements like oxygen or nitrogen.[9]

Tungsten, as many other transition metals, is reactive and easily getters residual gases of the processing chamber during deposition. A small amount of titanium is often added to tungsten to form a two-phase polycrystalline metallic alloy. Titanium (10–30 at. %) serves to improve the adhesive and corrosion resistive properties of tungsten. This alloy has been commonly adopted in semiconductor technology,[10] but again the importance of the impurity content in controlling grain boundary diffusion should be appreciated.[11] Rather than stuffing grain boundaries with impurities, another way to eliminate these rapid diffusion paths, is to use alloy compositions that tend to form an amorphous structure.[12] Amorphous alloys that have a high crystallization temperature, and often involve tungsten; Fe–W,[13] Ni–W,[14] Si–W,[15] and Zr–W[16] have been investigated as diffusion barriers. For these binary alloys, the formation of compounds between one or both of the barrier elements and the metallic overlayer or the substrate is the primary failure mechanism.

So far, nitrogen has appeared in tungsten-based diffusion barriers in three studies. (i) Nitrogen impurities have been assumed to be advantageous for good barrier performance of sputtered W between Si and Au.[17] (ii) Ti–W has been sputter deposited in a nitrogen-containing atmosphere with a significant resulting improvement of the barrier properties.[18] Whether the added nitrogen stuffs the grain boundaries or raises the barrier stability by actually forming transition metal nitrides, or both, is not presently known. (iii) In an investigation of the chemical reactivity of sputtered amorphous Ni–W films with aluminum, it was noted that when nitrogen was added, an amorphous Ni–N–W alloy was obtained and that the reactivity was reduced. The reason for this improvement is unclear.[14]

We consider here the simple case of the binary W–N alloy without other intentionally added elements. The motivations for this work are the ease with which W–N films can be deposited by sputtering of tungsten in an Ar–N_2 mixture, the good diffusion barrier properties of (nominally) elemental tungsten in comparison with most other metals, and the beneficial effects of nitrogen in stabilizing many transition metal barriers.[14,18,19]

Various forms of tungsten nitrides have been reported in literature, including cubic W_2N, hexagonal WN, and rhombohedral WN_2.[20] These compounds are not as stable as the nitrides of the titanium and vanadium groups; e.g., the heat of formation of W_2N is ~ -17 kcal/mol while that of TiN is ~ -80 kcal/mol.[21] Decomposition of tungsten nitrides has been reported at temperatures > 700 °C in vacuum, as well as upon exposure to water. However, tungsten nitrides do not dissolve in common mineral acids.[21] Published thin-film studies are, to our knowledge, limited to resistor applications[22] and to brief studies of structural,[23] optical,[24] and superconducting[25] properties.

The composition of our tungsten–nitrogen films was varied from W to $W_{35}N_{65}$. Single crystalline silicon substrates were used without any interposed contacting silicide layers.

*This paper was chosen from the symposium on Materials Interactions in Microelectronic Coatings to receive the Bunshah Award.

TABLE I. Abbreviations adopted for the samples of this study. Their structure is Si⟨100⟩/$W_{100-x}N_x$/metal overlayer.

Barrier and composition	Metal overlayer		
	Ag	Au	Al
W	Ag0	Au0	Al0
$W_{77}N_{23}$	Ag23	Au23	Al23
$W_{67}N_{33}$	Ag33	Au33	Al33
$W_{54}N_{46}$	Ag46	Au46	Al46, Al46a, Al46b
$S_{45}N_{55}$	Ag55	Au55	Al55
$W_{35}N_{65}$	Ag65	Au65	Al65

To test the diffusion barrier properties of the films, aluminum, gold, and silver were chosen for the metallic overlayers because of their importance in integrated circuit or solar cell applications as low resistivity metals. Gold and aluminum are also among the most difficult metals to keep from reacting with silicon, because of the existence of low eutectic temperatures (370 °C for Au–Si, 577 °C for Al–Si) and because of the high metallurgical reactivity of these two metals.

II. EXPERIMENTAL PROCEDURES

Silicon substrates of ⟨100⟩ orientation and of high electrical resistivity (900 Ω cm) were used. Before depositions, the substrates passed through organic cleaning and etching in a dilute HF solution.

All films of this study were deposited by reactive rf sputtering using planar magnetron cathodes of 7.5 cm diam. The system was equipped with an oil diffusion pump and a chiller trap, which were able to evacuate the chamber to a background pressure of $0.4–1.0\times10^{-6}$ Torr prior to deposition. The upper limit of this range was used unless noted in the text. Throttling the pumping line for the sputtering process increased the base pressure to $1.5–3.5\times10^{-6}$ Torr. The diffusion barrier layers of W and W–N were sputtered from a W target, placed in contact with the water cooled cathode, in Ar or in premixed Ar–N_2 gas ambients, respectively. The substrate holder was generally connected to the ground potential, but in some cases a dc bias voltage was applied to the holder. Films of W–N of five different compositions were prepared by changing the Ar:N_2 ratio in the premixed gas. The films of all five compositions and their metallic overlayer were deposited in the same vacuum cycle. For the W–N film depositions, a static sputtering mode was used, i.e., both the target and the substrate were stationary. The rotatable substrate holder was only used to move new substrates under the sputtering target between depositions. The vacuum cycle was completed by sputtering one of the overlayer metals (Ag, Au, or Al) in argon with the dynamic deposition mode; the substrates were cyclically passing beneath the orifice that was placed below the target to prevent shallow angle deposition. The rotation speed was about 2 rpm, and the path of the substrates was such that a net deposition rate of about one-tenth of the corresponding static rate resulted.

The specific samples are abbreviated in the text as shown in Table I and the corresponding sputtering parameters are given in Table II. The factor x in $W_{100-x}N_x$ gives the measured value of the nitrogen concentration of the sputtered films which has an uncertainty of a few at. %.

After deposition, the substrates were cleaved into pieces of about 1×1 cm^2 area and annealed at different temperatures (between 500–900 °C) for 30 min in an oil-diffusion pumped and liquid-nitrogen-trapped vacuum furnace. The pressure during annealing was below $\sim10^{-6}$ Torr. The resulting changes due to interdiffusion, reactions, and thermal mismatch were analyzed in several ways. Sheet resistances of the metal overlayers were measured with a four-point probe, mechanical changes were monitored by optical and scanning electron microscopy, and interdiffusion was analyzed by 2 MeV $^4He^+$ backscattering spectrometry. In some cases, x-ray diffraction and Auger electron spectroscopy were used to get additional structural information.

III. RESULTS

A. Sputtered W–N films

Properties of the tungsten–nitrogen alloy films used in this study are reported in detail elsewhere.[26] Some of the results relevant for the diffusion barrier application are given in Table III. The electrical resistivities are within an acceptable range for electronic applications when the electrical current flows predominantly through the barrier rather than along it. It is interesting to note that a certain range of nitrogen

TABLE II. Deposition parameters used for sputtering of W and W–N diffusion barriers, and for Ag, Au, and Al overlayers.

	Thickness (Å)	Argon pressure (10^{-3} Torr)	Nitrogen pressure (10^{-3} Torr)	rf power (W)	Deposition rate (Å/min)	Substrate bias (V_{dc})
W	800–900	10	...	400	690	...
$W_{77}N_{23}$	850–1050	9	1	400	590	...
$W_{67}N_{33}$	800–1050	8	2	400	550	...
$W_{54}N_{46}$	850–950[a]	6	4	400	500	...[b]
$W_{45}N_{55}$	1150–1200	4	6	400	375	...
$W_{35}N_{65}$	900–1000	2	8	400	230	...
Ag	2200–2800	3	...	400	375[c]	...
Au	3600–3900	3	...	500	380[c]	...
Al	1100–1300[a]	3	...	500	120[c]	−40

[a] Except Al46b: 1400 Å $W_{54}N_{46}$, 1540 Å Al.
[b] Except Al46a: −50 V_{dc}.
[c] Net deposition rate in dynamic sputtering.

TABLE III. Properties of sputtered W–N films.[a]

	Electrical resistivity ($\mu\Omega$ cm)	Phases identified[b] as deposited	650 °C[c] 30 min	800 °C[c] 30 min
$W_{77}N_{23}$	190	a-W–N	$W + W_2N$	W
$W_{67}N_{33}$	220	a-W–N	W_2N	W
$W_{54}N_{46}$	400	$W_2N(+x)$	$W_2N(+x)$	W
$W_{45}N_{55}$	2000	x	x	W
$W_{35}N_{65}$	4600	x	x	W

[a] Reference 26.
[b] Read camera x-ray diffraction.
[c] Annealing in $< 10^{-6}$ Torr vacuum, x = WN, WN_2?

partial pressures (8% to 23% of the total sputtering pressure of 10 mTorr in our case) yields amorphous films (*a*-W–N). This W–N system offers thus an opportunity to investigate grain boundary effects of diffusion barriers. The crystallization temperature of the amorphous W–N layers is about 620 °C unless the composition matches closely that of W_2N. In that case the film may crystallize at temperatures as low as 480 °C.[26] At 800 °C in vacuum, all films release nitrogen and only bcc tungsten can be seen in the resulting x-ray diffraction pattern. This is accompanied by a drop in electrical resistivity to $\sim 30\,\mu\Omega$ cm for all compositions. The bulk resistivity of bcc W is about $5\,\mu\Omega$ cm.

B. Sheet resistance and backscattering measurements of Si/W/metal and Si/W–N/metal samples

Silver, gold, and aluminum have low electrical bulk resistivities of about $2\,\mu\Omega$ cm. The sheet resistance R_s of a 2000 Å thick layer of such material is thus 0.1 Ω. By comparison, our tungsten–nitrogen barrier layers have $R_s \gtrsim 190\ \mu\Omega$ cm/1000 Å = 19 Ω, which is two orders of magnitude higher than that of the metal overlayer. Because the silicon substrates are of high resistivity (900 Ω cm), the sheet resistance of our barrier layer with overlayer samples is determined by the metal overlayer within an accuracy of ~1%. In cases of pure W barriers, the sheet resistances are somewhat more affected by the diffusion barrier (a few percent) than in cases of W–N. In reality, the measured sheet resistances after a sintering step at 500 °C and film thicknesses derived from backscattering spectra, lead to resistivity values of 2.1, 3.7, and 4.1 $\mu\Omega$ cm for Ag, Au, and Al films, respectively (without correcting for the underlayer W–N).

The stability of the sheet resistance of a metallization scheme is an important property and an indicator of metallurgical interactions, like chemical reactions or even grain boundary motion. A clear understanding of the results generally requires the support of other analytical techniques. We have measured the thermal stability of the sheet resistance of our samples, and have related the results to atomic depth profiles obtained by backscattering spectrometry.

In Fig. 1, the sheet resistances of annealed samples, normalized to the as-deposited value, are given for the silver samples (Ag0–Ag65). The first annealing step at 500 °C for 30 min decreases R_s by about 30% for all samples. That this is only a "sintering" effect of silver (grain growth, improved crystalline quality) is suggested by the indistinguishable backscattering spectra in the two cases. A similar reduction takes place for the other overlayer metals, too. All silver samples then remain unchanged up to an annealing temperature of 600 °C in both electrical and structural respects. Dissimilarities between samples, however, emerge at 700 °C. Ag23 and Ag46 are still unchanged at that temperature [see Figs. 1 and 2(b)], but for Ag0, Ag33, Ag55, and Ag65, the sheet resistance increases slightly and a small tungsten signal can be seen in backscattering [Fig. 2(a)] at high energies (~1.8 MeV) indicating that some tungsten exists now on the surface of the sample. That this is caused by cracks in the Ag layer is shown in the next section. Sample Ag0 with pure W barrier has a special behavior at 700 °C when compared to all those containing nitrogen in W. It is the interaction of W with silicon to form a nonuniform silicide, as can be seen in Fig. 2(a) from the modification of the edge of the Si signal (0.7–0.9 MeV) and of the low energy part of the W signal (1.3–1.5 MeV). Also silicon can now be seen on the sample surface (~1.1 MeV) probably through the cracks in Ag. No interaction of W–N with Si is seen at 700 °C in any sample. At 800 °C, all the silver samples fail by severe intermixing.

Unlike silver, gold has a low eutectic temperature of 370 °C with silicon. Because we used no masking or lithography steps to confine the area of the metal overlayer, metallurgical reaction effects can be seen to progress from the edges of our samples toward their center at high temperatures. However, a sufficiently large area was always preserved on which to make reliable measurements. The nor-

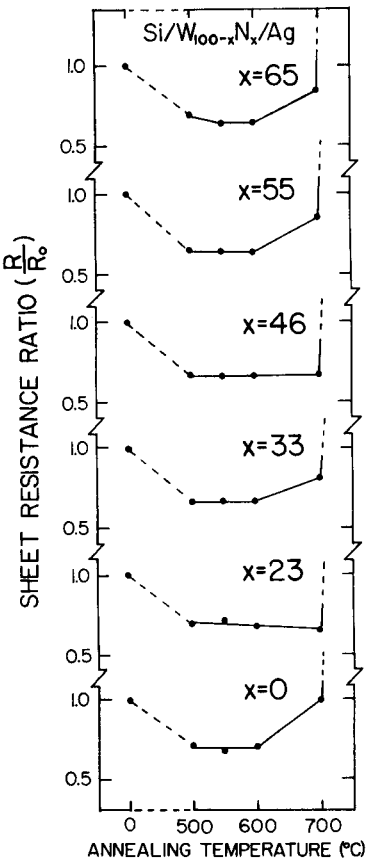

FIG. 1. Normalized sheet resistances of the $Si/W_{100-x}N_x/Ag$ samples as a function of vacuum annealing temperature (30 min). A slight increase in sheet resistance is seen at 700 °C for some samples. All barriers fail at 800 °C.

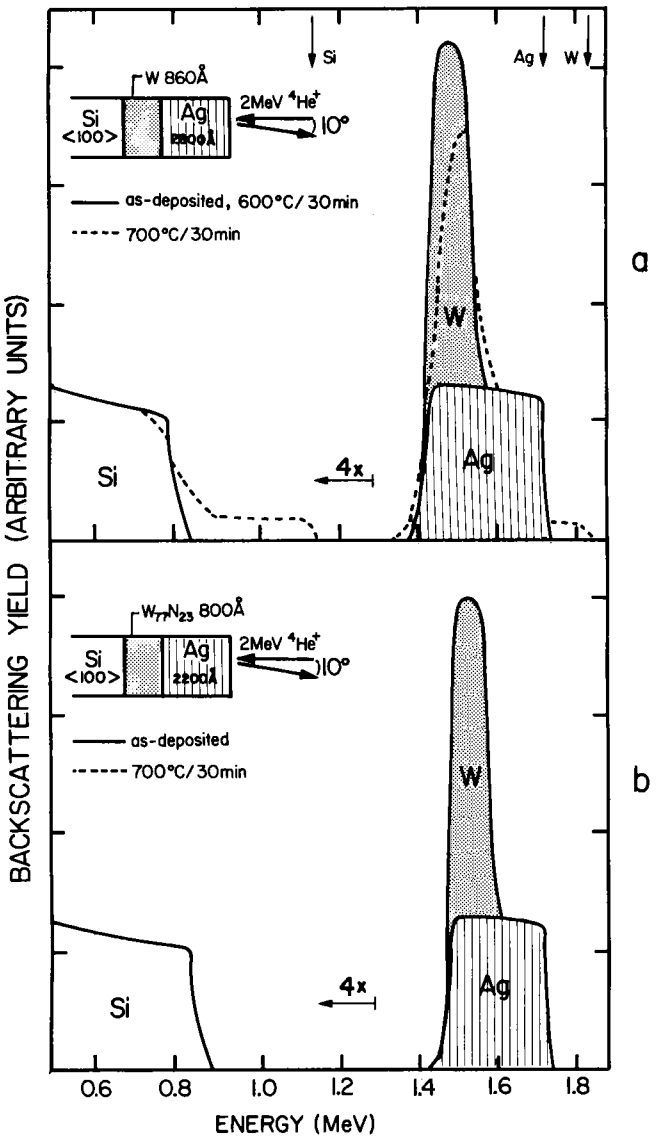

FIG. 2. Backscattering spectra show differences between $Si/W_{100-x}N_x/Ag$ samples after annealing at 700 °C. (a) The case with a pure W barrier shows W–Si intermixing. This sample also has cracks in the Ag layer so that W and Si can be seen on the sample surface. (b) $Si/W_{77}N_{23}/Ag$ is stable at 700 °C for 30 min.

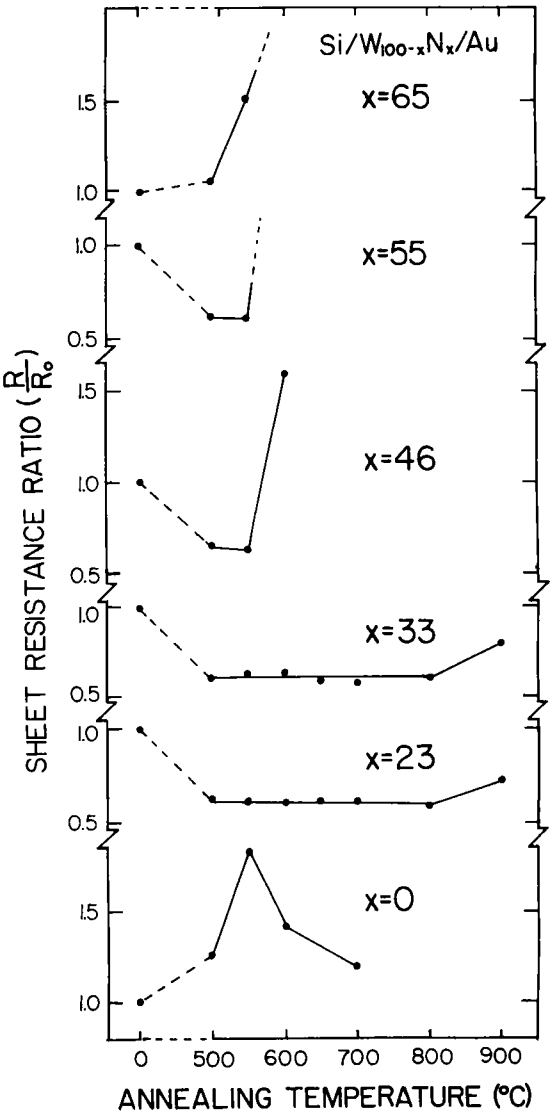

FIG. 3. Normalized sheet resistances of the $Si/W_{100-x}N_x/Au$ samples as a function of vacuum annealing temperature (30 min). Polycrystalline $W_{45}N_{55}$ and $W_{54}N_{46}$ barriers are stable up to 550 °C, and amorphous $W_{67}N_{33}$ and $W_{77}N_{23}$ even up to 800 °C. W and $W_{35}N_{65}$ are not effective diffusion barriers in this scheme.

malized sheet resistances of the gold samples (Au0–Au65) are shown in Fig. 3 as a function of annealing temperature. Large variations are seen in this case. At 500 °C already, the sputtered tungsten layer (sample Au0) cannot prevent a major degradation of the structure [see Figs. 3 and 4(a)]. The barriers $W_{77}N_{23}$ and $W_{67}N_{33}$ with an amorphous structure (see Table III) are clearly most effective for gold. At 800 °C, the sheet resistance is still unchanged, and no major interactions are seen by backscattering [Figs. 3 and 4(b)]. There is, however, a measurable increase in the backscattering yield between energies 0.7–1.2 MeV. As discussed later, this change is due to localized failure points of the diffusion barrier. Samples Au46, Au55, and Au65 have a polycrystalline barrier layer. Electrical and backscattering measurements show a decrease in the critical failure temperature from 600 to 500 °C with increasing nitrogen concentration in these polycrystalline nitrides.

An aluminum overlayer reacts with a tungsten barrier at 500 °C (30 min) in a nonuniform fashion. The sheet resistance increases, and W reaches the surface position. This behavior has also been reported in literature.[5,6] The localized diffusion of W is suppressed by adding nitrogen to the layer. Both sheet resistance and backscattering measurements show stability at 500 and 550 °C annealing steps [see Figs. 5 and 6(a)] for all Si/W–N/Al systems. Finally, at 600 °C, all the samples Al23, Al33, Al46, Al55, and Al65 degrade. In the course of our experimental studies, we produced two W–N barrier layers (Al46a and Al46b) that showed improved properties with respect to aluminum when compared to those shown in Figs. 5 and 6(a). In sample Al46a, the W–N layer was sputter deposited onto an electrically negatively biased (— 50 V) substrate. In sample Al46b, two conditions were changed: a better base vacuum (by a factor of 2) was used for the depositions, and a slightly extended deposition

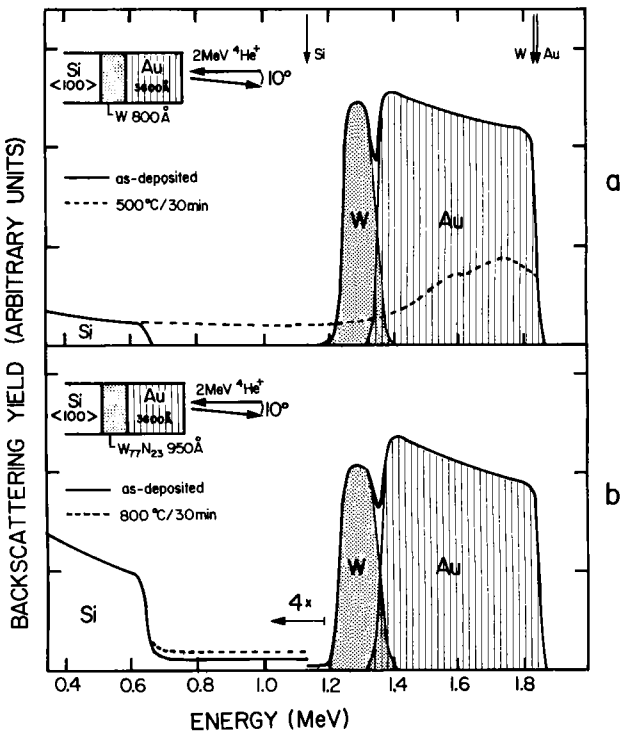

FIG. 4. (a) Backscattering spectrum shows total failure of the Si/W/Au sample after annealing at 500 °C for 30 min. (b) In the $Si/W_{77}N_{23}/Au$ sample, the integrity is maintained at 800 °C. Localized failures are observed, however (see yield increase between 0.7–1.1 MeV).

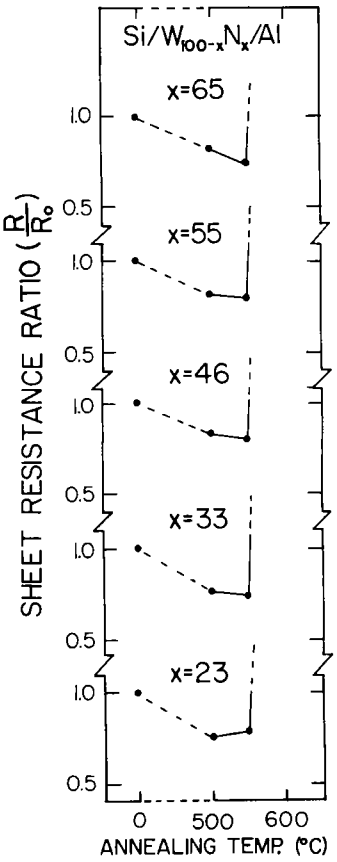

FIG. 5. Normalized sheet resistances of $Si/W_{100-x}N_x/Al$ samples as a function of vacuum annealing temperature (30 min). All barriers fail at 600 °C.

time increased the barrier thickness to 1400 Å. The sheet resistance measurements show a small rise in R_s for these samples at 600 °C, rather than a catastrophic failure; the corresponding backscattering spectra are shown in Figs. 6(b) and 6(c). All barriers in the samples whose spectra are shown in Fig. 6 (Al46, Al46a, and Al46b) were sputtered in the same nitrogen partial pressure and rf power, yielding polycrystalline W_2N films. Systematic studies of the effects of the bias voltage, the vacuum conditions, or the barrier thickness were not made. Such experiments seem worth carrying out.

C. Microscopy

Two clearly different kinds of structures can be seen on the annealed samples containing W or W–N diffusion barrier and a metal overlayer by inspecting them with an optical microscope. One of them seems to be related to thermal mismatch between the layers and the substrate. Localized loss of adhesion and delamination in one or both of the interfaces forms bubblelike characters at elevated temperatures. The other one is probably connected to defects in the diffusion barrier, giving rise to localized metallurgical reactions spots. Both of these defect types have been reported earlier in cases of TiN or HfN diffusion barriers.[27,28] The former of them may be fatal only if the diffusion barrier itself is delaminated from the substrate, because it leads to fracturing of the barrier at the edges of the characters[27] and finally to reactions between the substrate and the overlayer. On the other hand, if the overlayer only delaminates from the barrier surface and the barrier itself maintains its integrity, the process has no effect to the operation of the semiconductor devices underneath. The temperature ranges at which mechanical or chemical instability is seen with microscopy in the different samples, are given in Table IV.

To see in which interface delamination predominantly takes place, metal overlayers were chemically etched from some of the samples having surface bubbles. NH_4OH/H_2O_2—solutions were used for Ag and HCl/HNO_3—solutions for Au and Al etching. Sheet resistances of the etched samples were measured to confirm that only the overlayer was removed by the solutions, and that

TABLE IV. Optically detectable surface structures in Si/W–N/metal samples after 30 min annealing steps at different temperatures (T_a). 1 = thermal mismatch induced delamination patterns, 2 = same as 1 and localized chemical interactions (craters), and 3 = coarse surface due to large scale interactions.

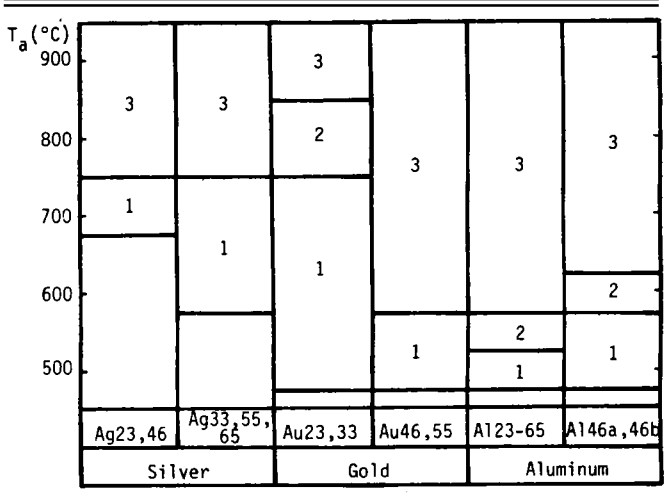

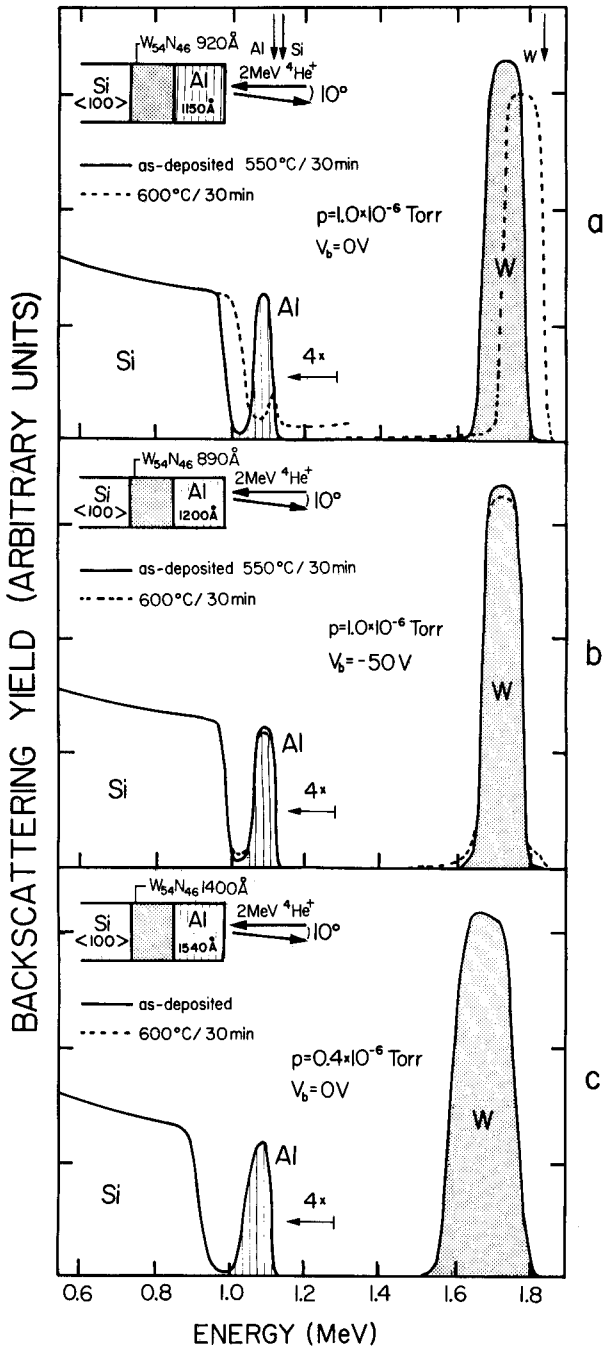

FIG. 6. Backscattering spectra of three $Si/W_{54}N_{46}/Al$ samples before and after vacuum annealing. Different conditions were used for W–N sputtering. Large scale in-diffusion of Al at 600 °C (a) is limited to localized spots when substrate bias voltage is used during sputtering (b), or by depositing in better base vacuum (c). In the last case, the analyzing beam doesn't hit the rarely appearing failure spots.

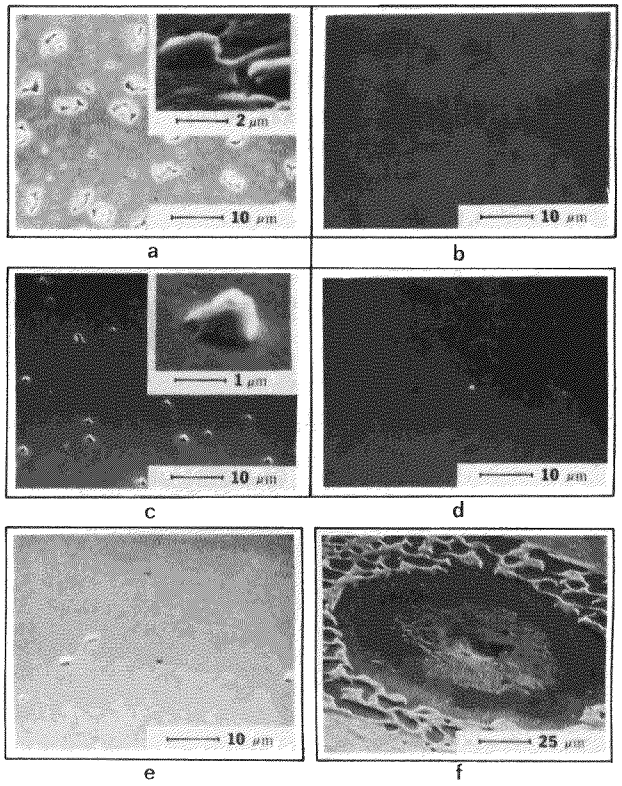

FIG. 7. SEM micrographs of annealed Si/W–N/metal samples before and after chemical etching of the metal overlayer. (a) Blistering and fracturing is seen in the $Si/W_{45}N_{55}/Ag$ sample after annealing at 700 °C. (b) Etching of Ag removes the characters. (c) Blistering is seen in the $Si/W_{77}N_{23}/Au$ sample after annealing at 600 °C (d) Etching of Au removes the characters. The few characters of the $Si/W_{67}N_{33}/Al$ sample annealed at 550 °C (e) are also removed by etching Al (not shown). (f) A typical localized failure point observed in Si/W–N/Au (and Si/W–N/Al) samples annealed above the eutectic temperature of the overlayer with silicon.

W–N was not attacked. SEM micrographs taken from these samples with and without overlayers are shown in Fig. 7. Silver samples blister at 700 °C, and most of them (Ag0, Ag33, Ag55, and Ag65) also undergo fracture at the edges of the bubbles, as seen very clearly under large magnification and tilted angle of the incident electron beam [see Fig. 7(a)]. The removal of silver also removes these bubbles showing that the $W_{45}N_{55}$ barrier layer of this sample is intact [Fig. 7(b)]. The same applies in the case of Au metallizations annealed at 600 °C [Fig. 7(c)]; the mechanical structures disappear upon Au etching [Fig. 7(d)]. The aluminum samples annealed at 550 °C are smoother having less numerous bub-

TABLE V. Properties of aluminum, silver, and gold in correlation with the critical failure temperature T_f of the Si/W–N/metal system.

Metal	Atomic number	Crystal structure	Lattice constant (Å)	Atomic radius (Å)	Ionic radius (Å)	Melting point (°C)	T_{eut} (w. Si) (°C)	T_f (°C)
Al	13	fcc	4.05	1.43	0.50(+3)	660	577	~575
Ag	47	fcc	4.09	1.44	1.26(+1)	962	830	~750
Au	79	fcc	4.08	1.46	1.37(+1)	1064	370	~850

bles of micrometer size than the Ag or Au samples just described [Fig. 7(e)]. Again, these mechanical structures are in the overlayer only so that the etched samples resemble that shown in Fig. 7(b). Figure 7(f) exemplifies catastrophic failure points that are observed in some samples annealed above the metal–silicon eutectic temperature (failure density is about $1/cm^2$).

IV. DISCUSSION

The effectiveness of W–N diffusion barriers depends on many things. In our studies the larger the atomic number of the overlayer element is, the higher critical failure temperatures T_f, can be achieved (meaning here the temperature at which the best W–N barrier composition totally fails as a barrier). This cannot be explained by differences in atomic radii for Ag, Au, and Al which are about the same. Only ionic radii increase in the same order as critical failure temperatures (see Table V). The metal/silicon eutectic temperature T_{eut} does not have a correlation with T_f, and only in one case (Al), the two temperatures roughly coincide. T_f follows the order of the melting points T_m of the metal overlayers so that the failures take place at temperatures of $\sim$80–95% of the absolute melting points of the overlayer metals. Chemical failure modes are, of course, possible like in the case of Si/TiN/Al in which Al can react with Ti ($TiAl_3$) and N (AlN).[28] Structural details of W–N layers are of primary importance, too. In polycrystalline diffusion barriers, the grain boundaries are a determining factor. Their detailed structure is not known for our W–N films which leads to speculative discussion.

Tungsten films sputtered in our system are good diffusion barriers between silicon substrate and a silver overlayer up to annealing cycles at 600 °C for 30 min. At 700 °C, improvements in barrier stability are achieved by adding nitrogen into tungsten which prevents the tungsten silicide formation. However, at this temperature, the adhesion of Ag to W or W–N is not sufficient to prevent localized delamination of the overlayer due to its large thermal expansion coefficient α. An additional layer between the barrier and the overlayer may be necessary to promote adhesion if high temperature processing is used after deposition. Values of α for some common semiconductor contact materials at room temperature are given in Table VI.

TABLE VI. Thermal expansion coefficients at room temperature for common semiconductor contact materials (in 10^{-6}/K) (see Refs. 21, 29, 30).

Si	2.5
GaAs	7
W	4.5
Ti	8.5
TiN	9
Ag	19
Au	14
Al	23

Tungsten layers sputtered in our system are not able to prevent the Au/Si eutectic formation at 500 °C. The thermal stability can be improved much by using W–N alloys instead of W. Especially the amorphous range of W–N compositions is effective as a gold diffusion barrier. Because only two of our sample compositions are good even at such high temperatures as 800 °C and because they are also the only ones with an amorphous barrier, it is appealing to relate the effectiveness of these layers to the absence of grain boundaries.[12] Surprisingly, however, crystallization to $W + W_2N$ or to single phase W_2N at 700 °C does not lead to degradation of the structure. Not even release of nitrogen from the W_2N phase at 800 °C results in interdiffusion. That these processes indeed take place like in the cases without metal overlayers[26] was confirmed by x-ray diffraction analysis. To get information about the redistribution of nitrogen, Auger depth profiling was used. No change was observed in the nitrogen signal up to annealing temperature of 800 °C. One thus comes to the conclusion that after this heat treatment, the barriers are composed of W crystallites with a high nitrogen concentration in their boundaries. These films are still effective barriers between Si and Au. Samples Au46, Au55, and Au65 have even more nitrogen in the barrier layer than the amorphous compositions, but they fail below 600 °C. Our analytical techniques are not able to resolve the detailed structure of grain boundaries, which could be helpful in explaining these phenomena.

In aluminum metallizations, temperatures around the Al/Si eutectic point seem to set a high threshold to surpass. In this case, no differences are seen between the properties of W–N barriers of different compositions, all of them being, however, superior to W without nitrogen. The microstructure of the W–N layers, being amorphous or polycrystalline (by Read camera x-ray diffraction), seems to be of limited importance here. This may indicate that the barriers fail by chemical reactions as has been reported to be the case for TiN and for some other interstitial compounds in a similar scheme.[28,31] A ternary Al–W–N phase diagram would be very helpful in estimating the reaction sequence. Destructive localized processes take place already at temperatures lower than 600 °C. Controlling the amount of impurities like oxygen and carbon seems to be of importance; our present experiments suggest that purer is better in the case of W–N diffusion barriers.

It is interesting to make comparisons between W–N and other interstitial alloys as diffusion barriers; TiN as the best studied case may serve as an example. The critical failure temperatures measured here are at least the same as those reported for TiN in similar systems.[27,32] W–N, however, offers some advantages over TiN. Stress-related problems that are quite common for TiN, are only observed for W–N samples with the highest nitrogen concentration ($W_{35}N_{65}$), never for most other compositions. To get quantitative values of intrinsic stress, $\sim$800 Å thick layers of TiN and $W_{67}N_{33}$ were sputtered onto thin cover glass slides (175 $\mu\Omega$ m thick) with deposition conditions adjusted according to the demands of diffusion barrier applications, but by fixing the deposition rate as well as the gas composition and pressure. For TiN, a substrate bias voltage was thus used,[27] but not in

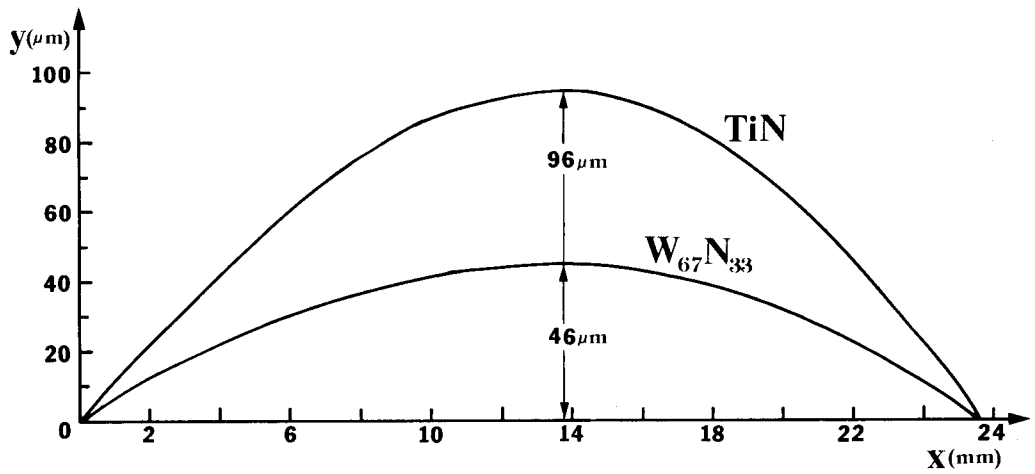

FIG. 8. Deflections of thin cover glass slides due to intrinsic stresses of 800 Å thick $W_{67}N_{33}$ and TiN films measured with Dektak profilometer. The average incremental stress in TiN is twice as large as in $W_{67}N_{33}$ in our case.

the case of amorphous $W_{67}N_{33}$. The deflections of the substrates due to intrinsic stresses in the sputtered films were measured with a Dektak profilometer. Both films proved to be in compression (see Fig. 8), but TiN more strongly than $W_{67}N_{33}$ by a factor of 2. The corresponding average inremental stress values derived as in Ref. 33 are 5.9 GPa (5.9×10^{10} dyn/cm^2) for TiN and 2.7 GPa (2.7×10^{10} dyn/cm^2) for $W_{67}N_{33}$. These values may have both material and deposition-related components. At elevated temperatures, thermal stresses are created. The thermal expansion coefficients (see Table VI) for our W–N films are not known, but that no delamination effects are seen in the Si/W–N interface indicates either low thermal stresses or good adhesion, both properties being favorable.

W–N films are practically insoluble in H_2SO_4, HNO_3, and HCl, but precautions should be made in exposing these materials to water, since W_2N has been reported to react with H_2O.[21] The films can be photolithographically patterned in a W etch [34 g KH_2PO_4, 13.4 g KOH, 33 g $K_3Fe(CN)_6$, H_2O to make 1 liter[34]], but at a reduced rate when compared to W.

V. CONCLUSIONS

The commonly used simple trick of adding nitrogen into the deposition atmosphere of diffusion barriers also proves useful for tungsten barriers. For all metal overlayers studied (Ag, Au, and Al) improvement in thermal stability is achieved when using W–N diffusion barriers on silicon substrates instead of mere tungsten. These materials are practical alternatives for high temperature electronic applications tolerating short (30 min) treatments at temperatures as high as 800 °C.

ACKNOWLEDGMENTS

We thank J. L. Tandon, Applied Solar Energy Corporation, City of Industry, California, for his help in SEM analysis, A. E. Morgan, Signetics Corp., Sunnyvale, California, for AES analysis, and R. Gorris, Caltech, for technical assistance. We are also indebted to A. A. Jaecklin, Brown Boveri & Cie, Baden, Switzerland, for the gift of high purity Si substrates. This work was financially supported in part by the Department of Energy through an agreement with the National Aeronautics and Space Administration and monitored by the Jet Propulsion Laboratory, California Institute of Technology, Pasadena, California, and by the U. S. Army, Electronics Technology and Devices Laboratory (ERADCOM), Ft. Monmouth, New Jersey.

[a] Permanent address: Technical Research Centre of Finland, Otakaari 7B, SF-02150 Espoo, Finland.

[1] S. Swirhun, K. C. Saraswat, and R. M. Swanson, IEEE Electron Device Lett. **EDL-5**, 209 (1984).
[2] S. P. Murarka, *Silicides for VLSI Applications* (Academic, New York, 1983).
[3] M. Wittmer, J. Vac. Sci. Technol. A **2**, 273 (1984).
[4] M-A. Nicolet, Thin Solid Films **52**, 415 (1978).
[5] I. Krafcsik, J. Gyulai, C. J. Palmstrom, and J. W. Mayer, Appl. Phys. Lett. **43**, 1015 (1983).
[6] C. Y. Ting and M. Wittmer, Thin Solid Films **96**, 327 (1982).
[7] G. J. van Gurp, J. L. C. Daams, A. van Oostrom, L. J. M. Augustus, and Y. Tamminga, J. Appl. Phys. **50**, 6915 (1979); G. J. van Gurp and W. M. Reukers, *ibid.* **50**, 6923 (1979).
[8] M. Bartur and M-A. Nicolet, Appl. Phys. Lett. **39**, 822 (1981).
[9] M-A. Nicolet and M. Bartur, J. Vac. Sci. Technol. **19**, 786 (1981).
[10] R. S. Nowicki and M-A. Nicolet, Thin Solid Films **96**, 317 (1982).
[11] J. E. Baker, R. J. Blattner, S. Nadel, C. A. Evans, Jr., and R. S. Nowicki, Thin Solid Films **69**, 53 (1980).
[12] M-A. Nicolet, I. Suni, and M. Finetti, Solid State Technol. **26**, 129 (1983).
[13] I. Suni, M-A. Nicolet, C. S. Pai, and S. S. Lau, Thin Solid Films **107**, 73 (1983).
[14] M. F. Zhu, F. C. T. So, and M-A. Nicolet, Thin Solid Films (to be published).
[15] J. D. Wiley, J. H. Perepezko, J. E. Nordman, and K.-J. Guo, IEEE Trans. Ind. Electron. **IE-29**, 154 (1982).
[16] M. F. Zhu, F. C. T. So, E. T-S. Pan, and M-A. Nicolet, Phys. Status Solidi A **86**, 471 (1984).
[17] R. S. Nowicki, Solid State Technol. **25**, 127 (1982).
[18] R. S. Nowicki, J. M. Harris, M-A. Nicolet, and I. V. Mitchell, Thin Solid Films **53**, 195 (1978).
[19] R. S. Nowicki and I. Wang, J. Vac. Sci. Technol. **15**, 235 (1978).
[20] H. J. Goldschmidt, *Interstitial Alloys* (Plenum, New York, 1967).
[21] G. V. Samsonov and I. M. Vinitskii, *Handbook of Refractory Compounds* (IFI/Plenum, New York, 1980).
[22] J. R. Rairden, III, U. S. Patent No. 3 655 544 (11 April 1972), and U. S. Patent No. 3 714 013 (30 January 1973).
[23] P. T. Dawson and S. A. J. Stazyk, J. Vac. Sci. Technol. **20**, 966 (1982).
[24] L. A. Cherezova and B. P. Kryzhanovskii, Opt. Spectrosc. **34**, 234 (1973).
[25] F. M. Kilbane and P. S. Habig, J. Vac. Sci. Technol. **12**, 107 (1975).
[26] K. Affolter, H. P. Kattelus, and M-A. Nicolet, Spring Meeting of the Materials Research Society, San Francisco, 1985.
[27] I. Suni, M. Mäenpää, M-A. Nicolet, and M. Luomajärvi, J. Electrochem.

Soc. **130**, 1215 (1983).
[28]M. Wittmer, J. Appl. Phys. **53**, 1007 (1982).
[29]*CRC Handbook of Tables for Applied Engineering Science*, edited by R. E. Bolz and G. L. Tuve (Chemical Rubber, Cleveland, 1970).
[30]S. K. Ghandhi, *VLSI Fabrication Principles Silicon and Gallium Arsenide* (Wiley–Interscience, New York, 1983).
[31]R. Beyers, R. Sinclair, and M. E. Thomas, J. Vac. Sci. Technol. B **2**, 781 (1984).
[32]N. Cheung, H. von Seefeld, and M-A. Nicolet, Proc. Symp. Thin Film Interfaces and Interactions **80-2**, 323 (1980).
[33]D. W. Hoffman and J. A. Thornton, Thin Solid Films **40**, 355 (1977).
[34]T. A. Shankoff and E. A. Chandross, J. Electrochem. Soc. **122**, 294 (1975).